Journal of Applied Research and Technology

www.jart.icat.unam.mx
Journal of Applied Research and Technology 17 (2019) 186-194

Original

Nickel (II) sorption from aqueous media by *Agave salmiana* as biosorbent

D. M. Sánchez-Nava[a,b], H. López-González[a]*, M. T. Olguín[a], S. Bulbulian[c]

[a]*Instituto Nacional de Investigaciones Nucleares, Gerencia de Ciencias Básicas, Departamento de Química, Carretera México-Toluca S/N La Marquesa Ocoyoacac Estado de México C. P. 52750.*
[b]*Tecnológico de Estudios Superiores de San Felipe del Progreso, Avenida Tecnológico S/N, Ejido de San Felipe del Progreso, 50640 San Felipe del Progreso,*
[c]*Instituto de Ciencias Aplicadas y Tecnología, Universidad Nacional Autónoma de México, Circuito exterior S/N, Cd. Universitaria, C.P. 04510, México, Ciudad de México*

Abstract: In this work, the removal of nickel from aqueous solutions by *Agave salmiana* was investigated. For this purpose the removal of this heavy metal (Ni^{2+}) was carried out in a batch system as a function of contact time, pH, and the initial concentration of the metallic specie in solution. The sorption data were fitted to pseudo-first order and pseudo-second order kinetic models to found the parameters which describe the processes. It was found that the maximum sorption of the Agave for Ni^{2+} was at pH 10 and pseudo-second order kinetic model well described the biosorption behavior of this heavy metal by the non-living biomass. Furthermore, the maximum sorption capacity obtained from the isotherm was 10 mgNi/gAgave.

Keywords: *Agave salmiana*, sorption, nickel

1. INTRODUCTION

Nickel (Ni) is a heavy metal that is used in various industrial processes and it is found as Ni^{2+} in aquatic systems. Chemical factors which can affect the chemical speciation of nickel include pH and the presence of organic and inorganic compounds. This metal is found in the water due to the chemical and physical degradation of rocks and soils, deposition of atmospheric particulate matter and discharges from industries. Among the sources of nickel in water are primary nickel production, metallurgical processes, fossil fuel combustion, incineration, chemical and catalyst production. The routes of entry of the nickel to human beings is through inhalation, ingestion and cutaneous absorption (EPA,1986).

Ingestion of nickel by humans is relatively high compared to other toxic elements, and it could be explained by the utensils used to prepare food. Cutaneous absorption of Ni is related to hypersensitivity and skin damage (EPA, 1986; ATSDR,1997). It is reported that its ingestion, more than the maximum permissible limit causes various types of acute and chronic disorder, such as severe harm to lungs and

* Corresponding author.
E-mail address: hilario.lopez@inin.gob.mx (H. López-González).
Peer Review under the responsibility of Universidad Nacional Autónoma de México.

kidney, gastrointestinal distress (for example nausea, vomiting, diarrhea), pulmonary fibrosis and renal edema (Abdullah & Prasad, 2010; Akhtar, Iqbal, & Iqbal, 2004; EPA, 1986; ATSDR,1997). The World Health Organisms has recommended a guide value of 0.07 mg/L in drinking water (WHO, 2005).

Efficient and innocuous environmental technologies are needed to reduce the heavy metal content in wastewaters into acceptable level of affordable cost. The alternative and innovative wastewater treatment techniques as well as the recovery technologies have been focused on the use of biological materials such as algae, fungi, yeast, and bacteria for the metal removal. These technologies have gained importance during recent years (Abdullah & Prasad, 2010; Akhtar et al., 2004; Johnson, Jain, Joshi, & Prasad, 2008; Gebresemati, Gabbiye, Sahu, 2017). Biosorption is a potential alternative for the treatment of industrial effluents and aquatic ecosystems contaminated with heavy metals (Abdullah & Prasad, 2010; Akhtar et al., 2004; Johnson et al., 2008). Thus, it is important to develop methods for separating Ni(II) from aqueous media using non-living biomasses considering also their simplicity, versatility and the low cost. Among these biomaterials the *Agave salmiana* which is and endemic plant from Mexico, could be used to remove heavy metals from polluted water (Akhtar et al., 2004). Therefore in this work, the sorption of the Ni(II) from aqueous media by the *Agave salmiana* as non-living biomass was investigated taking account the contact time, pH and the initial concentration of this heavy metal in solution.

2. EXPERIMENTAL

2.1 BIOMATERIALS

The dried *Agave salmiana* (AS) (Figure 1) was collected in San Jerónimo Acazulco, Mexico. It is cut into small pieces, grounded and sieved to select particles of 20 mesh. This material was washed with distilled water (AS-N) and then, with a 10^{-4} M hydrochloric acid solution (J. T. Baker) until no green–brown colour was observed in the washing solutions. Thereafter, the material was dried again in the stove at 70 °C and stored in a desiccator prior to use. The sample was labeled as AS-H.

2.2 CHARACTERIZATION

2.2.1 Morphology and elemental composition

Samples were directly mounted onto metal holders, with the particles adhered on a conducting substrate. Analysis by SEM was performed with a Philips XL-30 electron microscope to obtain the morphology of the biomass components at different amplifications. Elemental analyses were obtained by EDS with a DX-4 probe at 500 X.

Fig. 1. *Agave salmiana* a) before conditioning b) after conditioning.
Figure (a) taken from https://thpix.com/media/560909328571475081
Figure (b) taken from http://magueytlax.blogspot.com/p/materia-prima-del-maguey.html

2.2.2 Mineral composition and crystallinity

The X-ray diffraction patterns of the samples were obtained using a Siemens D5000 diffractometer with Cu Kα radiation and a diffracted beam monochromator. The X-ray tube was operated at 35 kV and 20 mA. Crystalline compounds were conventionally identified with Powder diffraction files (PDF).

2.2.3 Functional groups

FT-IR spectra in the 4000–400 cm^{-1} range were recorded for the AS-N and AS-H samples before and after the Ni(II) sorption, at room temperature using a Nicolet Magna-IR 550 FT-IR. Samples were prepared using the standard KBr pellets method.

2.2.4 Texture

Specific surface areas, total pore volume and mean pore diameter of solid samples were determined using the N_2 Brunauer-Emmett-Teller (BET) method. The analyser BELSORP-28SA was used for this purpose. Before the analyses, the samples were dried at 300 °C during 2 h and degassed at 70 °C for 2 h. The pore radius was calculated according to Gregg and Sing (1982) considering the following equation:

$$\frac{V_p}{S_{BET}} = \frac{r_p}{2} \quad (1)$$

Where Vp represents the pore volume, S_{BET} is the specific surface area and r is the pore radius.

2.2.5 Surface charge

The pH of the zero charge point (pH_{pzc}) was obtained using batch equilibration technique (Faria, Orfao, & Pereira, 2004). The samples were introduced into glass bakers containing 40 mL of 0.01 M NaCl solution with 150 mg of biosorbent. The initial pH was adjusted from 2 to 12 by adding a few drops of 0.1 M HCl or 0.1 M NaOH. The mixtures were shaken for 24 h at 20 °C and the final pH values of the filtered suspensions were measured using MeterLab PHM290-pH meter. Plots of $pH_{initial}$ *vs.* pH_{final} were constructed and the pH_{PZC} was determined from the intersection of these curves.

2.3 UPTAKE OF NI(II)

Batch experiments were carried out at 20 °C to determine the uptake kinetics by shaking closed vials from 5 min to 24 h with a mixture of 100 mg of AS-H and aliquots of 10 mL of a 25 ppm Ni solution at pH 5.5. A Cole Parmer Polystat, model 12050-00 temperature circulator bath was used for this experimentation. The residual nickel solutions were then filtered to separate the phases. The supernatant liquid was recovered and analyzed. Similar experiments were carried out considering: (1) Ni solutions of 25 mg L^{-1} at 20 °Cand pH values from 2 to 12 in contact with the non-living biomass during 24 h and (2) Ni solutions of different concentrations (from 5 to 600 mg L^{-1}) in contact with the non-living biomass during 24 h, at pH of 5.5 and20 °C. All of the experiments were performed in duplicate.

The amount of Ni(II) adsorbed per unit mass of the sorbent and the corresponding percentage were calculated by:

$$q_e = \frac{(C_0 - C_e)V}{m} \quad (2)$$

$$R = \frac{(C_0 - C_e)}{C_0} X\ 100 \quad (3)$$

where q_e $(mg \cdot g^{-1})$ is the amount of Ni(II) ions adsorbed by AS-H, C_o and C_e are the initial and equilibrium nickel concentrations in solution $(mg \cdot L^{-1})$ at any time, respectively, V is the volume of solution (L), and m is the amount of biomass (g). R represents the percentage of Ni(II) sorbed by AS-H.

2.4 DETERMINATION OF NICKEL IN AQUEOUS SOLUTION

A stock solution of Ni ($NiCl_2 \cdot 6H_2O$, analytical grade reagent), from J.T. Baker chemicals company, was prepared with distilled water to obtain a 600 mg L^{-1}. Before and after nickel adsorption by AS-H, the solutions were diluted, and the concentrations were determined using a GBS 932 Plus atomic absorption spectrophotometer at 232.0 nm considering a calibration curve from 0.25 to 5 mg/L giving a correlation coefficient of 0.997.

3. RESULTS AND DISCUSSION

3.1 CHARACTERIZATION

3.1.1 Morphology and elemental composition

Figure 2 shows the images at different magnifications of the non-living biomass *Agave salmiana* treated with 10^{-4} M HCl solution (AS-H), where it can be seen that this biosorbent is granular, with porosity and has elongated components. No changes were observed in the morphology of the samples after they were in contact with the nickel solution.

The main components of the AS-H were: C 35.0 wt.%, O 45 wt. %, Ca 19 wt. %, and Mg 1.1 wt. %, and when this material was in contact with the nickel solutions (AS-H-Ni), the presence of nickel was clearly observed (0.22 wt. %).

3.1.2 Mineral composition and crystallinity

Figure 3 shows the XRD patterns of the AS-H and AS-N samples for comparison purpose. The AS-N sample shows a reflexion at 15.0 in 2-theta degrees. This reflexion is attributed to the whewellite compound (PDF file 00-020-0231). This crystalline phase corresponds to the calcium oxalate hydrate ($CaC_2O_4{\cdot}H_2O$) with a monoclinic crystalline system (Hidalgo-Reyes, Caballero-Caballero,Hernández-Gómez, & Urriolagoitia-Calderón, 2015). Calcite reflexions also were observed at 29.0 in 2-theta degrees (Figure 3). Furthermore, there are reflexions with low intensity and great amplitude, characteristic of amorphous materials.

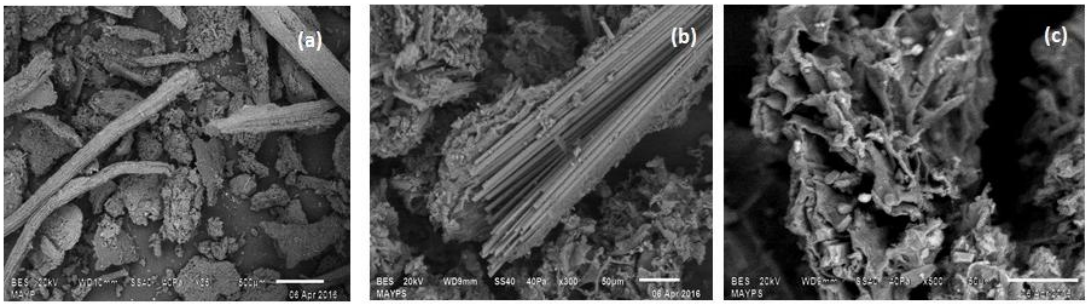

Fig. 2. SEM images at different magnifications of the *Agave salmiana (AS-H) sample, a) 35X b) 300X and 3 c) 500X.*

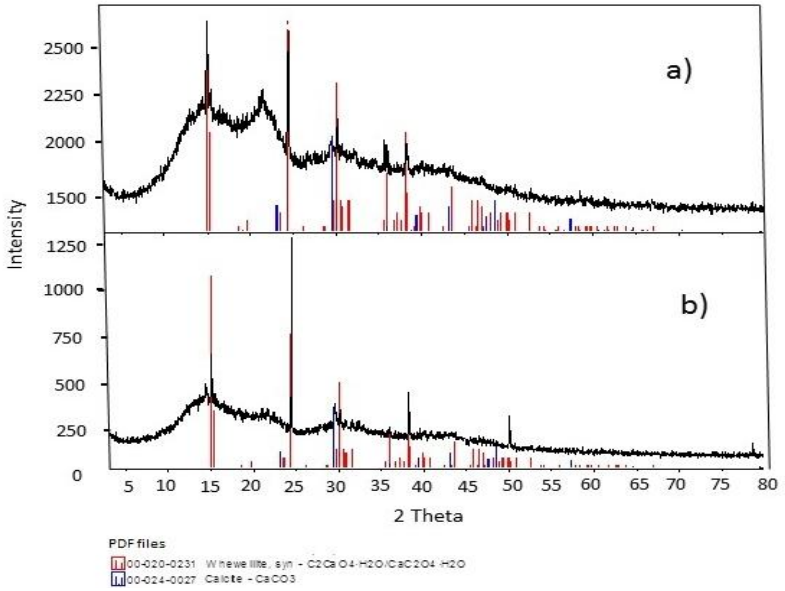

Fig. 3. XRD patterns of a) AS-N and b) AS-H.

3.1.3 Functional groups

Figure 4 shows the FT-IR spectra of AS-N and AS-H samples. The absorption bands observed were identified as follows: a wavenumber of 3428 cm^{-1} indicates the presence of OH groups on the AS-N and AS-H samples. The 1628 cm^{-1} band is a result of CO stretching mode, conjugated to a NH deformation mode and is indicative of amide band. The CO or CN groups were assigned to the band at 1049 cm^{-1}.Thus, this spectrum reveals the presence of several functional groups which could be bonded to Ni(II) chemical species on the AS-H surface, among others carboxylic and hydroxylic groups. The AS-H presents similar bands to those of AS-N (Table 1). No modification in the IR spectra of AS-H after the Ni(II) uptake were observed. *Agave americana* presents a similar IR spectra (Kestur et al., 2013) to that of *Agave salmiana.*

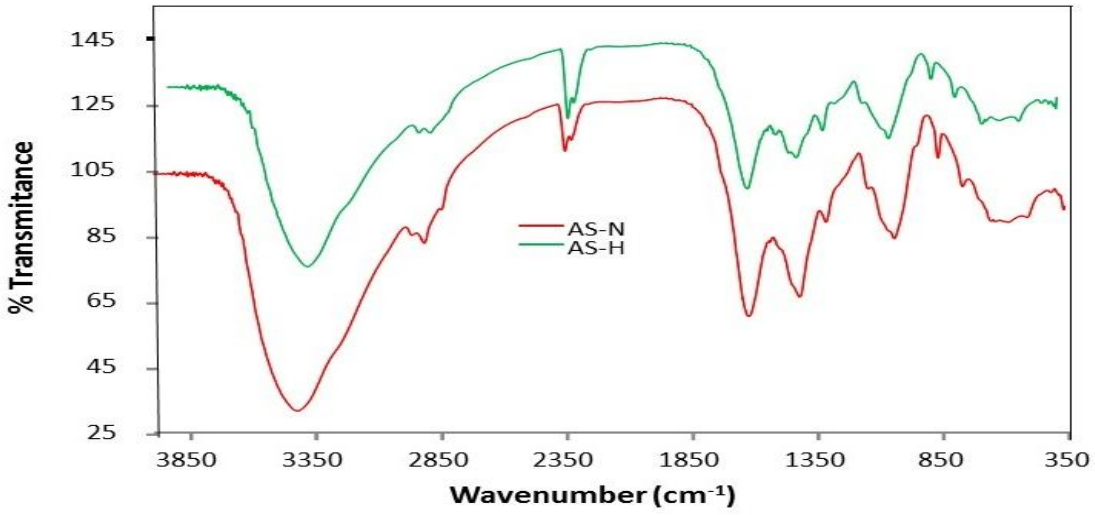

Fig. 4. Infrared spectrum of samples AS-N and AS-H.

Table 1. Assigned absorption bands from the FT-IR spectra of AS-N and AS-H.

Wavenumber (cm^{-1})		Groups
AS-N	AS-H	
3428.14	3427.73	Hydrogen bonded O-H stretching
3428.14	3427.73	Attributed to cellulose I_p
2972.58	2973.3	C-H stretching vibration from CH and CH_2 in cellulose and hemicellulose
2923.67	2927.65	NA
1629.4	1627.65	Carbonyl C=O stretching of the acetyl groups of hemicelluloses
1544.62	1544.6	NA
Not present	1508.2	NA
Not present	1457.42	O-H in plane bending
1427.84	1427.92	CH_2 symmetric bending
1322.16	1319.33	C-O group of the aromatic ring in polysaccharides
Not present	1151.31	Anti-symmetric stretching C-O-C
1049.69	1049.55	CO and O-H stretching vibrations which belongs to polysaccharide in cellulose
877.57	877.57	β-Glycosidic linkages between the monosaccharides
775.35	777.28	NA
667.45	667.45	Out of plane vibrations involving ring structure
Not present	651.47	NA
596.35	596.35	C-OH bending
518.85	518.85	NA

NA: absorption band no assigned

3.1.4 Texture

Table 2 displays the specific surface areas, total pore volumes and mean pore diameters for the AS-N and AS-H samples. The specific surface area of the *Agave salmiana* (AS-N) was 0.7954 m^2/g and of the *Agave salmiana* treated with 10^{-4} M HCl solution (AS-H) was 1.084 m^2/g. It can be observed that the treatment of AS-N with HCl solution, increases the specific area in 26 %.

Table 2. Specific surface area, total pore volume and pore diameter of untreated and treated *Agave salmiana*

Sample	Specific surface area (m^2/g)	Total pore volume (cm^3/g)	Pore diameter (nm)
AS-N	0.7954	0.1814	56.345
AS-H	1.084	0.00736	27.129

The total pore volume and pore diameter is low for AS-H than AS-N samples. These variations in the textural characteristics of the samples could be attributed to the washing with the HCl solution.

The specific surface area affects the adsorption behavior. Greater specific surface areas lead to greater adsorption of the pollutants species on the solid. This result occurs because a large number of active sites are available for sorption in solids with high specific surface areas.

3.1.5 Surface charge

Depending of the surface charge of the non-living biomass AS-H, the cationic chemical species of Ni(II) could interact with the surface of the adsorbent material to remove this heavy metal from the aqueous media. The pH_{pzc} found for AS-H was 7.4. Therefore at pH below this value, the surface of the AS-H has positively charged sites and adsorbs anions and at pH higher than this value, the surfaces have negatively charged sites and can adsorb cations. In the case of the present work the contact between the Ni (II) aqueous solutions and the adsorbents materials (AS-H) were done at initial pH of 5.5. Then, the mechanism to remove these heavy metals from water by AS-H cannot be preferentially through coulombic interactions. The chemical speciation of Ni(II) as well as the textural characteristics of AS-H could be also involved in the adsorption mechanisms.

3.2 UPTAKE OF NI(II)

3.2.1 Sorption kinetics

Figure 5 shows the Ni(II) uptake by AS-H as a function of time. In the first 60 min a fast Ni(II) sorption was observed and the equilibrium of the sorption process was reached at 300 min.

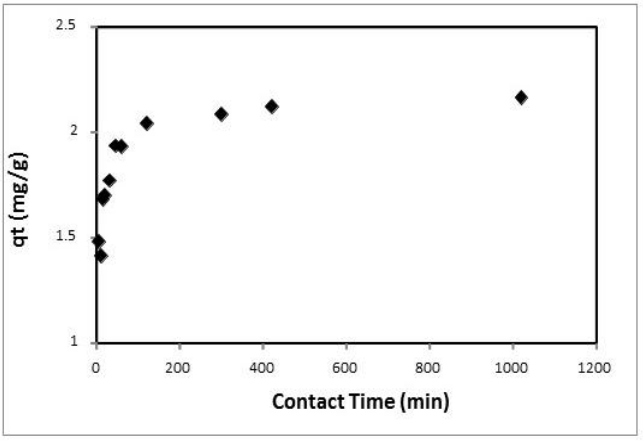

Fig. 5. Effect of contact time on Ni(II) sorption by the *Agave salmiana* treated with hydrochloric acid (AS-H).

The sorption capacity of AS-H for Ni(II) was of 2.04 mg/g, representing a removal of 90.4%.

The experimental results were fitted to the second-order model to describe the nickel adsorption kinetics by *Agave salmiana*. This model has been applied to describe the adsorption kinetics of heavy metals by other types of biosorbents (Ho & McKay, 1999).

The pseudo-second-order kinetic model has generally been considered for heterogeneous systems where the sorption mechanism is attributed to chemical sorption. The pseudo-second-order model is generally expressed as:

$$\frac{dq_t}{d_t} = k(q_e - q_t)^2 \quad (4)$$

where k is the rate constant of sorption $(g \cdot mg^{-1} \cdot min^{-1})$, q_e is the amount of solute

time t $(\text{mg} \cdot \text{g}^{-1})$. After integration and applying boundary conditions of $t = 0$ to $t = t$ and $q_t = 0$ to $q_t = q_t$, the equation is:

$$\frac{t}{q_t} = \frac{1}{kq_e^2} + \frac{1}{q_e}t \quad (5)$$

The nickel adsorption experimental data fitted well to the pseudo-second-order kinetic model ($r^2 > 0.999$) for AS-H (Figure 6). This behavior indicates that chemisorption plays an important role in the removal of nickel by AS-H. The pseudo-second-order rate constant (k_2) was 0.07550 $\text{g} \cdot \text{mg}^{-1}\text{min}^{-1}$. The sorption capacities (q_e), obtained by applying the pseudo-second-order kinetic model, was similar to that obtained experimentally for AS-H (2.17 $\text{mg} \cdot \text{g}^{-1}$). In the biosorption kinetic process of Ni(II), the pore volume and the size of the pore of the biomass could be playing a role in the diffusion of the heavy metal to favor the interaction with the specific sorption sites.

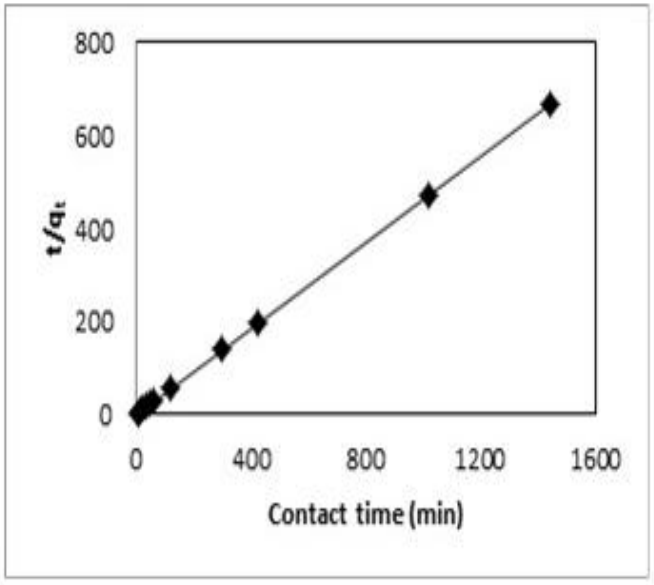

Fig. 6. Pseudo-second order kinetic model applied to the sorption of Ni(II) by AS-H.

3.2.2 pH effect

It was observed that at pH values between 4 and 12, maximum Ni(II) retention (R) was achieved with AS-H (approximately 99.5 %) (Figure 7) and drastically the sorption was decreased at pH 2. Into the pH range between 6.0 and 10.0 and considering a nickel concentration of 25 ppm, Ni(II) ions exist mainly (99.5%) as $Ni(OH)_2$. The cation Ni^{2+} exists at pH values <2.0. In the pH range from 5 to 9, $Ni(OH)^+$ and $Ni(OH)_2$ can coexist in various proportions, and from pH values from 9 to 12, only $Ni(OH)_2$ can be observed in solution considering the chemical equilibrium diagram for Ni(II) obtained by Medusa program (Puigdomenech, 2004). Thus, Ni^{2+}, $Ni(OH)^+$ and $Ni(OH)_2$ are the chemical species that may be adsorbed on the sorption sites from the *Agave salmiana (AS-H).*

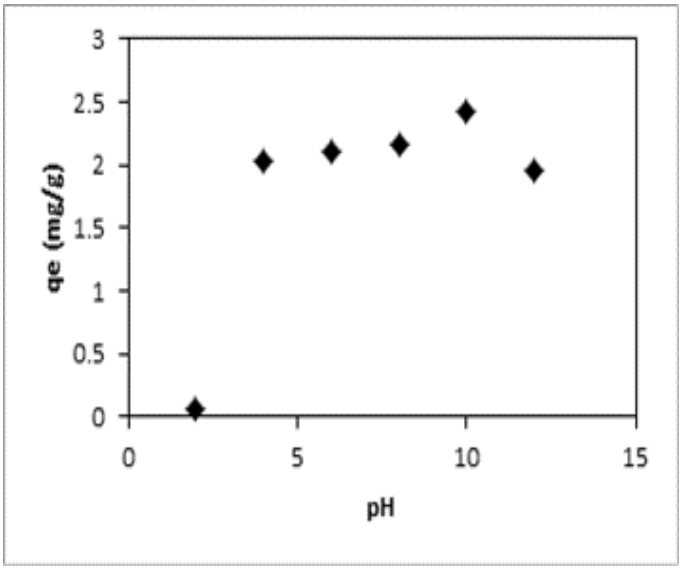

Fig. 7. Effect of pH on nickel adsorption by AS-H.

The mechanism to explain the Ni(II) sorption by *Agave salmiana* at basic pH values could be through the oxygen containing groups (e.g. carboxylic and phenolic) from AS-H (Velazquez-Jimenez, Pavlick, & Rangel-Mendez, 2013). At basic pH value, the predominant species of Ni (II) is $Ni(OH)_2$. It is possible that Ni (II) could be precipitated on the surface of AS-H.

$$2(\equiv \text{R-COO}^-) + \text{Ni}^{2+} \leftrightarrow (\equiv\text{R-COO})_2\text{Ni} \quad (6)$$

$$\equiv \text{R-COO}^- + \text{Ni(OH)}^+ \leftrightarrow \equiv\text{R-COONiOH} \quad (7)$$

$$\equiv \text{R-COOH} + \text{Ni(OH)}_2 \leftrightarrow \equiv\text{R-COOH}^{\cdots}\text{Ni(OH)}_2 \quad (8)$$

The pH was measured in the solutions before and after the Ni (II) sorption process and the pH variation was low.

3.2.3 Sorption Isotherms

Figure 8 shows the sorption of Ni(II) as a function of initial concentration. It was observed that the sorption of Ni(II) increases until a little inflection was reached at approximately 200 mg/L. The adsorption capacity increased continuously and the saturation of the *Agave salmiana* with nickel(II) was not observed. The maximum sorption capacity of the AS-H for Ni(II) was 10 mg/g. This value can be associated with the specific surface area of the sorbent, the chemical speciation in solution and the interaction of Ni with the functional groups of the constituents of the material.

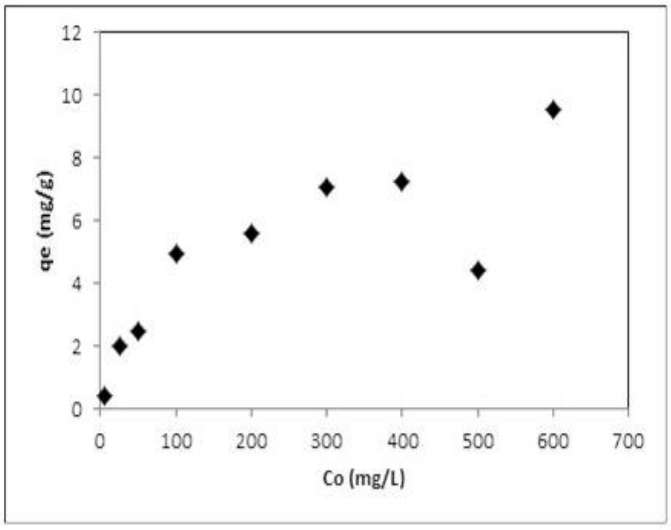

Fig. 8. Effect of the initial Ni(II) concentration in solution on the sorption of this metallic specie by AS-H.

4. CONCLUSIONS

Chemical treatments performed to raw *Agave salmiana* modified with hydrochloric acid (AS-H) shows no changes in its morphology, with respect to the *Agave salmiana* before treatment. The pH of the zero charge point is close to neutrality and the specific area slightly increases, when the AS-N is modified with hydrochloric acid to obtain AS-H. The equilibrium of the Ni(II) sorption by (AS-H) is reached at 300 min. The sorption capacity (q_e) of AS-H for Ni (II) is 2.17 mg/g, when the experimental data was fitted to pseudo second order kinetic model. The biosorbent (AS-H) mostly removes the Ni (II) from the aqueous medium at pH value of 10. The maximum sorption capacity of AS-H for Ni(II) is 10 mg/g. The *Agave salmiana* modified with acid solution is an acceptable biosorbent to remove Ni(II) from aqueous solution.

ACKNOWLEDGEMENTS

The authors thank to Consejo Nacional de Ciencia y Tecnología (CONACYT project 254665); by support this work. The authors also thank the valuable contributions of Dr. J. Serrano-Gómez to this paper.

CONFLICT OF INTEREST

The authors have no conflicts of interest to declare.

REFERENCES

Abdullah, M. A., & Prasad, A. D. (2010). Biosorption of nickel (II) from aqueous solutions and electroplating wastewater using tamarind (Tamarindus indica L.) bark. *Australian Journal of Basic and Applied Sciences*, 4(8), 3591-3601.

Akhtar, N., Iqbal, J., & Iqbal, M. (2004). Removal and recovery of nickel (II) from aqueous solution by loofa sponge-immobilized biomass of Chlorella sorokiniana: characterization studies. *Journal of hazardous materials*, *108*(1-2), 85-94.

ATSDR, Agency for Toxic Substances and Disease Registry. (1997). *Toxicological Profile for Nickel (Update)*. Public Health Service, U.S. Department of Health and Human Services, Altanta, GA.
Retrieved from https://www.atsdr.cdc.gov/toxprofiles/tp15.pdf

EPA, US Environmental Protection Agency. (1986). Health assessment document for nickel, EPA/600/8-83/012F, *National Centre for Environmental Assessment*, Office of Research and Development, Washington, DC. Retrieved from https://nepis.epa.gov/Exe/ZyPDF.cgi/20007SR6.PDF?Dockey=20007SR6.PDF

Faria, P. C. C., Orfao, J. J. M., & Pereira, M. F. R. (2004). Adsorption of anionic and cationic dyes on activated carbons with different surface chemistries. *Water Research*, *38*(8), 2043-2052.

Gebresemati, M., Gabbiye, N., Sahu, O. (2017). Sorption of cyanide from aqueous medium by coffee husk: Response surface methodology. *Journal of Applied Research and Technology*, *15*(1), 27–35.

Gregg S. J., & Sing K. S. W. (1982). Adsorption, Surface Area and Porosity. 2nd Edn *86*(19). Academic Press Inc, London.

Hidalgo-Reyes, M., Caballero-Caballero, M., Hernández-Gómez, L. H., & Urriolagoitia-Calderón, G. (2015). Chemical and morphological characterization of Agave angustifolia

Ho, Y. S., & McKay, G. (1999). Pseudo-second order model for sorption processes. *Process biochemistry*, 34(5), 451-465.

Johnson, T. A., Jain, N., Joshi, H. C., & Prasad, S. (2008). Agricultural and agro-processing wastes as low cost adsorbents for metal removal from wastewater: A review. *Journal of Scientific and Industrial Research*, 67, 674-685.

Kestur, G, S., Flores-Sahagun, T. H. S., Dos Santos L.P., Dos-Santos, J., Mazzaro, I., Mikowski, A. (2013). Characterization of blue agave bagasse fibers of Mexico. *Composites Part A: Applied Science and Manufacturing*, *45*, 153-161.

Puigdomenech,I.(2004). HYDRA (Hydrochemical Equilibrium-Constant Database) and MEDUSA (Make Equilibrium Diagrams Using Sophisticated Algorithms) Programs. *Royal Institute of Technology*, Stockholm.

Velazquez-Jimenez, L. H., Pavlick, A., & Rangel-Mendez, J. R. (2013). Chemical characterization of raw and treated agave bagasse and its potential as adsorbent of metal cations from water. *Industrial Crops and Products*, *43*, 200-206.

WHO, (2005). Nickel in Drinking-water Background document for development of WHO Guidelines for Drinking-water Quality © World Health Organization, 15-16. WHO/SDE/WSH/05.08/55.

Figure (a) of page 187 Retrieved (mes día, año), from http://search.eb.com,https://thpix.com/media/560909328571475081

Figure (b) of page 187 Retrieved (mes día, año), http://magueytlax.blogspot.com/p/materia-prima-del maguey.html